

# On repellers in quasi-periodically forced logistic map system

Tsuyoshi Chawanya<sup>1, a)</sup> and Takafumi Sakai<sup>1</sup>

*Graduate School of Information Science & Technology, Osaka University, Toyonaka, JAPAN.*

(Dated: 3 March 2014)

We propose a method to identify and to locate "repellers" in quasi-periodically forced logistic map (QPLM), using a kind of Morse decomposition of nested attracting invariant sets. In order to obtain the invariant sets, we use an auxiliary 1+2-dimensional skew-product map system describing the evolution of a line segment in the phase space of QPLM. With this method, detailed structure of repellers can be visualized, and the emergence of a repeller in QPLM can be detected as an easily observable bifurcation in the auxiliary system. In addition to the method to detect the repellers, we propose a new numerical method for distinguishing a strange non-chaotic attractor (SNA) from a smooth torus attractor, using a correspondence between SNAs in QPLM and attractors with riddled basin in the auxiliary system.

PACS numbers: 05.45.Ac,02.30.Oz,02.60.Cb

Keywords: strange non-chaotic attractor; non-autonomous systems; bifurcation

**The topological structure of invariant sets as well as its variation (bifurcation) is one of the most basic and essential issues for understanding the behavior of a dynamical system. However, it is sometimes not easy to obtain invariant sets in non-autonomous systems, and that might make our understanding of those systems rather limited. In this paper we propose a method to identify and to locate repellers in quasi-periodically forced logistic map system, and exhibit the obtained images of repellers and bifurcation diagrams. It would be helpful for developing better understanding of mechanisms for the emergence of complex behaviors in quasi-periodically forced systems from dynamical system point of view.**

## I. INTRODUCTION

Quasi-periodically forced systems could be considered as one of the simplest class of "essentially non-autonomous" dynamical systems. In this class of systems, surprisingly complex dynamical phenomena, including rather common existence of strange non-chaotic attractors(SNA), were reported in early 1980s<sup>1-3</sup>. Since then the feature and the mechanism of such phenomena have been extensively studied by many researchers with various background, and related phenomena have been uncovered in relatively wide variety of systems<sup>4-10</sup>. Major part of the theoretical researches on the phenomena have been done mainly for the cases with systems with "forced" invariant set induced by something like symmetry<sup>14-21</sup>. On the other hand, also for the systems without such forced invariant sets, rigorous results are obtained however mainly in reversible 1+1-dimensional

systems: the existence of SNA is indicated for the case where the existence of continuous attractor is excluded by topological constraint<sup>11,12</sup> and the emergence of SNA at non-uniform saddle-node bifurcation is proven<sup>13</sup>. As for higher dimensional and/or irreversible systems, also where large part of the numerical studies have been done, there still many phenomena which have not been understood clearly.

When a quasi-periodic external force is applied to such systems that possibly exhibit chaotic behavior even without external forcing, it seems natural to expect that unstable invariant sets with complicated structure would play essential role in the dynamics<sup>22,23</sup>. In quasi periodically forced circle map system with relatively strong modulation (thus it is no longer reversible), existence of such complicated structure is indicated using densely distributed winding number of the orbits<sup>24</sup>. Also in numerical researches, repelling invariant sets with complicated structure are observed, for example, as a basin boundaries between two distinct attractors, and the boundary crisis has been identified as one of the routes to SNA. Thus such repelling invariant sets are considered to be directly relevant with the emergence of SNA at least for such cases.

In some other cases, the existence of repelling sets is also strongly suggested from observation of the parameter dependence of the size or the smoothness of the attractor (i.e., crisis-like drastic enlargement of an attractor or "fractalization" of a torus), while there seem to be no visible basin boundary in its neighborhood. In such cases it is not trivial task to identify and to locate such presumed repellers. One possible approach to locate such invariant sets is to consider a perturbation to the invariant sets in the system without external forcing. However, this method is applicable only for limited class of invariant sets (i.e., a torus or composition of multiple tori). Another useful approach is to approximate the quasi-periodic forcing with periodic one<sup>25,26</sup>, and thus approximate 1+1-dimensional skew-product system with 1-parameter family of 1-dimensional autonomous

<sup>a)</sup>Electronic mail: chawanya@ist.osaka-u.ac.jp

systems. This method, known as rational approximation (RA) method, have been used as a major tool to observe such invariant sets in numerical researches. It has been used for the classification of the bifurcation to create SNA in QPLM<sup>27-32</sup>, and corresponding types of bifurcation are observed also in QP-forced higher dimensional systems<sup>33-35</sup>. Though the observed features of the “repeller” obtained in RA are consistent with the qualitative changes of the behavior of the attractors on the whole, RA cannot reproduce the topological structure of the genuine “repeller” verbatim, and the correspondence of the bifurcations in QP-forced systems and those obtained by RA is somewhat obscure.

In this report, we propose a method to locate and to obtain the images of repellers in QP-forced logistic map system(QPLM) including those with non-trivial structures, and exhibit some of the numerical results obtained with this method. Our results are consistent with the bifurcation scenario that have been inferred from RA method or from direct observation of the attractors, and provide some novel perspective to bifurcation phenomena where various repellers are involved.

Our method is presented in section 2. We introduce an auxiliary dynamical system describing the evolution of a segment, that is given as a 1+2 dimensional skew-product map system, and describe outline of the method to identify “repeller” of the QPLM. Some details of the algorithm is given in the appendix. Some of the numerical results obtained with this method are demonstrated in section 3, including detailed phase diagram exhibiting a complicated bifurcation structure near TDT(torus doubling termination) critical point, as well as images of repellers with non-trivial structure. Summary and short discussion will be given in the last section.

## II. METHOD

In this section, we will explain our method to obtain the images of “repellers” in QPLM. In the first place, we introduce concrete form of the system and auxiliary “segment map”, a 1+2- dimensional skew-product map that describes the evolution of a “segment” in the phase space of QPLM. Then we describe the method to obtain repellers in QPLM. Some technical details of the algorithm to obtain the images of repellers, together with a method to distinguish SNA from “smooth” torus will be given in appendix.

### A. QPLM and “segment map”

Here we consider the quasi-periodically forced logistic (quadratic) map in the following form,  $M|\Omega \rightarrow \Omega, (\Omega := T^1([0, 1]) \times \mathbf{R}), M(\theta_n, x_n) = (\theta_{n+1}, x_{n+1})$

$$\begin{aligned} \theta_{n+1} &= (\theta_n + \omega) \bmod 1, \\ x_{n+1} &= a - x_n^2 + \epsilon \cos(2\pi\theta_n). \end{aligned} \quad (1)$$

$a$  and  $\epsilon$  are treated as control parameters, and  $\omega$  is fixed as  $(\sqrt{5} - 1)/2$  in this paper.

In order to examine the stability of a point in  $\Omega$ , it would be a natural approach to consider the temporal evolution of its neighborhood. Regarding the trivial neutral stability in the  $\theta$  direction, it seems reasonable to think about the evolution of a vertical segment that contains the target point. Fortunately the evolution of a vertical segment can be written concretely as a (1+2)-dimensional piece-wise polynomial skew-product map system.

Thus here we introduce an auxiliary “segment map” system, given as  $\tilde{M} | \tilde{\Omega} \rightarrow \tilde{\Omega}, \tilde{\Omega} = T^1([0, 1]) \times (\mathbf{R} \times \mathbf{R}_+), \mathbf{R}_+ = \{x \in \mathbf{R} | x \geq 0\}, \tilde{M}(\theta_n, z_n, w_n) = (\theta_{n+1}, z_{n+1}, w_{n+1})$

$$\begin{aligned} \theta_{n+1} &= (\theta_n + \omega) \bmod 1, \\ z_{n+1} &= \begin{cases} a - z_n^2 - w_n^2 + \epsilon \cos(2\pi\theta_n), & (|z_n| \geq w_n) \\ a - (|z_n| + w_n)^2/2 + \epsilon \cos(2\pi\theta_n), & (|z_n| < w_n) \end{cases} \\ w_{n+1} &= \begin{cases} 2|z_n|w_n, & (|z_n| \geq w_n) \\ (|z_n| + w_n)^2/2, & (|z_n| < w_n) \end{cases} \end{aligned} \quad (2)$$

Here  $\theta$  is the “phase” of the external force as in the QPLM(1).  $z$  and  $w$  correspond to the center position and the half-length of the segment respectively. Although the derivative of this map has discontinuity on  $z = 0$ , we have observed no symptom of pathological phenomena due to this discontinuity.

Note that, the subspace of zero-length segments ( $\tilde{\Omega}_0 = \{w = 0\} \subset \tilde{\Omega}$ ) is kept invariant by the map  $\tilde{M}$ , and the restriction of  $\tilde{M}$  on  $\tilde{\Omega}_0$  could be naturally identified with QPLM ( $M$  on  $\Omega$ ).

We sometimes call a subset of the phase space with common  $\theta$  value as a “fiber” (both for QPLM and for the segment map system). For a point  $u = (\theta, z, w) \in \tilde{\Omega}$ , the length of the corresponding segment in  $\Omega$  ( $= 2w$ ) is written as  $\text{length}(u)$ . For a point  $u = (\theta, z, w)$  in  $\tilde{\Omega}$ , we let  $\underline{u}$  to represent a set (segment)  $\{(\theta, x) \in \Omega | z - w \leq x \leq z + w\}$ . Similarly, for  $U$  which is a subset of  $\tilde{\Omega}$ , let  $\underline{U}$  stands for  $\bigcup_{u \in U} \underline{u} \subset \Omega$ . We call  $\underline{U}$  as the “shadow” of  $U$ . For an invariant set (that may or may not be an attractor)  $X \in W$  where  $W$  may be either  $\Omega$  or  $\tilde{\Omega}$ , we let  $B(X)$  denote the basin of attraction  $\{u \in W | \omega(u) \subset X\}$ , where  $\omega(u)$  denotes the  $\omega$ -limit set of the orbit starting from  $u$ .

### B. A method to locate repellers

Now let us describe the outline of the method to detect and to locate “repellers”. Our basic strategy is to find a set of points that are transversely unstable and non-wandering, using the map describing temporal evolution of a line segment.

As for the transverse stability of a point, we observe asymptotic behavior of an orbit (of the segment map) starting from a segment (with positive length) containing the point, and check if the length of the segment would

converge to 0 or not. If it converges to 0, that indicates no transversely unstable point is contained in the initial segment. On the other hand, if the length of the orbit starting from the segment has a positive limsup value, transversely unstable point(s) presumably exist in the initial segment.

The asymptotic behavior of the orbit of the segment map gives some information about the recurrence property of the points in the initial segment as well. As the  $\omega$ -limit set of an orbit of the segment map is an invariant set, its shadow determines a corresponding invariant set of the original QPLM. If the initial segment (i.e., a segment in QPLM corresponding to the shadow of the initial point of the segment map) is a subset of this invariant set, there should exist non-wandering points in the initial segment.

Thus we are interested in such point ( $p$ ) that satisfies

- $\omega$ -limit set of any orbits (of  $\tilde{M}$ ) starting from a point corresponding to non-zero length segment containing the point  $p$  is detached from  $w = 0$  plane,
- the shadow of the  $\omega$ -limit set contains the point  $p$

Above mentioned  $\omega$ -limit set for starting point corresponding to sufficiently short segments is expected to be one of the attractors of the segment map. Let  $A$  denote the attractor. The ensemble of orbits starting from a neighborhood of the original point  $p$  should be dense in the shadow of the attractor  $A$ . Thus the shadow of the attractor  $A$  could be regarded as a “basin of repulsion” of the repelling non-wandering point  $p$ .

There can be multiple repelling non-wandering points with the common “basin of repulsion”. The set of those repelling non-wandering points consist a transitive set. Thus the set as a whole could be identified as a “repeller”. We let  $R(A)$  denotes a repeller with “basin of repulsion”  $A$ .

Basically what we try to obtain is a image of the section of repellers on a target fiber. In order to do this, we try to carry out the following steps.

- Obtain the list of pull back attractors of the segment map on the target fiber,
- Find pull back attractors that correspond to a segment whose proper subset corresponds to another pull back attractor,
- Look for such points which are in the shadow of the outer attractor and whose corresponding  $\omega$ -limit set does not belong to any of inner attractor’s shadow.

The obtained set of points would be the section of the repeller whose basin of repulsion is given by the shadow of the outer attractor. In practice, we try to obtain the image of multiple sections of the repellers using the information of pull back attractors on one fiber. The detail of the procedure is described in the appendix.

It should be noted that a pull back attractor on a fiber does not simply correspond to a section of the attractor in autonomous 2-dimensional system.<sup>36</sup> If  $A \subset \Omega$  is an asymptotically stable attractor of  $M$  in the view the 2-dim autonomous system, boundary of  $A$  would consist of graph(s) of continuous and piece-wise smooth function of  $\theta$ . In such cases, the intersection of  $A$  with a certain fiber  $\{\theta = c\}$  should coincide with a pull back attracting set on the fiber (which may consists of multiple pull back attractors). On the other hand, for the cases with SNA, although pull-back attractor(s) for almost all fibers can be obtained just like the above case, the shape of their union over the fibers is not continuous. Thus SNA does not simply correspond to an asymptotically stable attractor of the 2-dimensional autonomous systems.

It is not easy to distinguish these two types of pull back attractors from simple observation. For the case of SNA, however, there should exist a repelling orbit (that should be a part of a repeller) in arbitrarily small neighborhood of the pull back attractor<sup>37</sup>. Thus we could expect that there exist trajectories of  $\tilde{M}$  starting from a point in an arbitrarily small neighborhood of an “SNA” but finally attracted to another attractor (of  $\tilde{M}$ ) that corresponds to the basin of repulsion of the repeller which is located in touch with the attractor(SNA). Thus, it is expected that SNAs exhibit a kind of sensitivity of final state against arbitrarily small perturbation in the neighborhood of the attractor in  $\tilde{M}$ , like those attractors with “riddled” basin<sup>16,38</sup>. We try to detect this presumed type of sensitivity of final state in  $\tilde{M}$  expected for SNAs, by checking whether a small perturbation for  $w$  component of  $\tilde{M}$  would make the destination of the trajectory to another attractor (in  $w > 0$  region) or not. Thus we introduce a “perturbed” version of segment map  $\tilde{M}^+$ , given as  $\tilde{M}^+ = \tilde{W}^+ \circ \tilde{M}$  where  $\tilde{W}^+ | \tilde{\Omega} \rightarrow \tilde{\Omega}$ ,  $\tilde{W}^+(\theta, z, w) = (\theta, z, \min\{w, \delta^+\})$ , where  $\delta^+$  denotes the amplitude of the perturbation. ( $\delta$  is set as  $5.0 \times 10^{-7}$  in the examples shown in this report.)

### III. NUMERICAL RESULTS

In this section, we present some of the numerical results, namely, phase diagrams in  $(a, \epsilon)$ -plane and visualized images of attractors and repellers for some selected parameter values.

The obtained phase diagram (Fig.1) seems similar to those obtained in the preceding studies. However, since our criterion to identify an attractor as SNA is different from those used in the preceding studies (based on the divergence of the estimated phase sensitivity), the position of the obtained borderline between smooth attracting torus and SNA has some discrepancy. It would be notable that we observed no SNA near the border of the boundary crisis which is associated with the disappearance of bounded attractor in the bump-like region near  $(a, \epsilon) = (1.2, 0.42)$  (as is shown in box (c)), which is consistent with the natural expectation that SNA appears

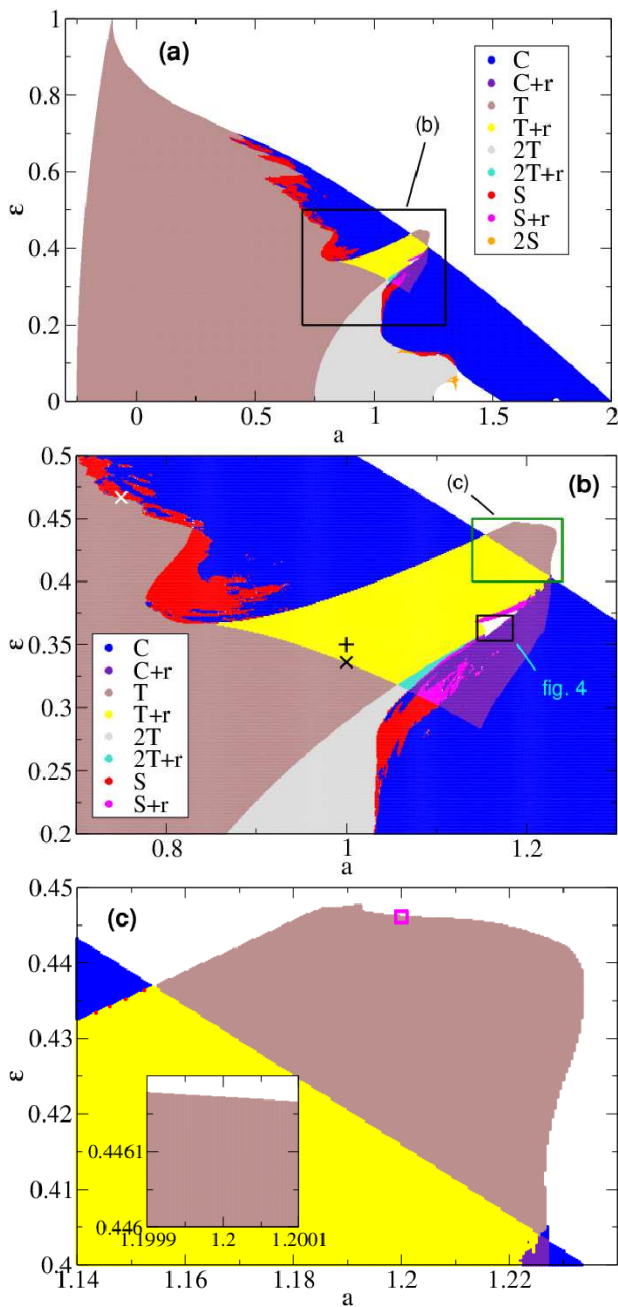


FIG. 1. Phase diagram in  $a$ - $\epsilon$  plane

Marks in the box (b) indicate parameter values corresponding to the following figures. Black star for fig. 2, black  $\times$  for fig. 3, white  $\times$  for fig. 6. Those plots are obtained with mesh size  $(\Delta a, \Delta \epsilon)$  taken as  $(0.002, 0.002)$  for (a),  $(0.001, 0.001)$  for (b),  $(0.0005, 0.0002)$  for (c) and  $(0.000002, 0.000001)$  for the inset of (c). The observed type of the attractor or the repeller is indicated with color as illustrated in the legend box in box (b). C, T, 2T and S respectively stand for chaotic, torus, period 2 tori and strange non-chaotic attractor, and “+r” indicates the existence of a “non-trivial” repeller which is not a part of the basin boundary with other attractors.

only AT the boundary crisis for such cases.

An example of the repellers with non-trivial structure (observed as “ring shaped” repellers in RA method) is exhibited in Fig. 2. Besides the apparently fractal layered structure, thin apertures can be observed in the rim of the rings (in boxes b and c). These thin apertures are mapped to the large gap near  $\theta = 0.35$  (indicated by a two-way arrow in box a), after 15 (for box b) and 28 (for box c) iterations.

The above result suggests that the repeller has a family of infinitely many apertures (with progressively thin widths), and thus when adequately coarse grained it could appear to consist of finite number of chunks. Thus the approximation for the repeller obtained by RA could be a good approximation for the repeller in quasi-periodically forced system, in spite of the fact that the set of finite number of rings cannot be invariant in the quasi-periodically forced system.

In the next figure (Fig. 3), we chose the parameter near the emergence of the ring-like shaped repeller, and visualized the shape of the repeller and the attracting invariant set corresponding to the basin of repulsion of the repeller. Sequence of inward spikes are observed in the boundary curve of the basin. We think that these spikes are a symptom of a non-uniform saddle-node bifurcation, where the attractor of  $\tilde{M}$  (which corresponds to the basin of the ring-like shaped repeller) collide with a saddle. Thus it is surmised that, at the bifurcation of the disappearance of the repeller, the boundary would touch the last component of the repeller on infinitely many fibers simultaneously, while on typical fibers the repeller of QPLM with fractal-like structure is still retained. Thus it is conjectured that the repeller would have strictly positive lyapunov exponent even at the onset.

An interesting repetitive bifurcation structure has been reported near the torus doubling termination (TDT) critical point<sup>39,40</sup>. Near this critical point, multiply nested structure of invariant sets is observed as shown in Figs.4 and 5. The obtained result is consistent with coexistence of multiple noisy attractors with different scales<sup>40</sup> and also with the features of the parameter dependence of the attractor<sup>4</sup>, i.e., the birth of SNA via internal crisis like behavior with decreasing  $a$  and via fractalization like behavior with increasing  $a$ .

In the next figure (Fig. 6), the parameter is set as  $(a, \epsilon) = (0.75, 0.46672)$ , a little after the onset of SNA by “fractalization” on the path corresponding to the one investigated by Kaneko and Nishikawa<sup>3,28</sup>. We can see a kind of fractal like complicated structure with some apparent smoothness, however, the images of the repeller is “dirty” due to apparently superimposed irregular vertical stripe like structure. We think that the repeller would be dense in its basin of repulsion due to these stripes and correspondingly the basin of SNA in  $\tilde{M}$  should be riddled, while structures with some smoothness would be apparent as far as we observe finite number of fibers.

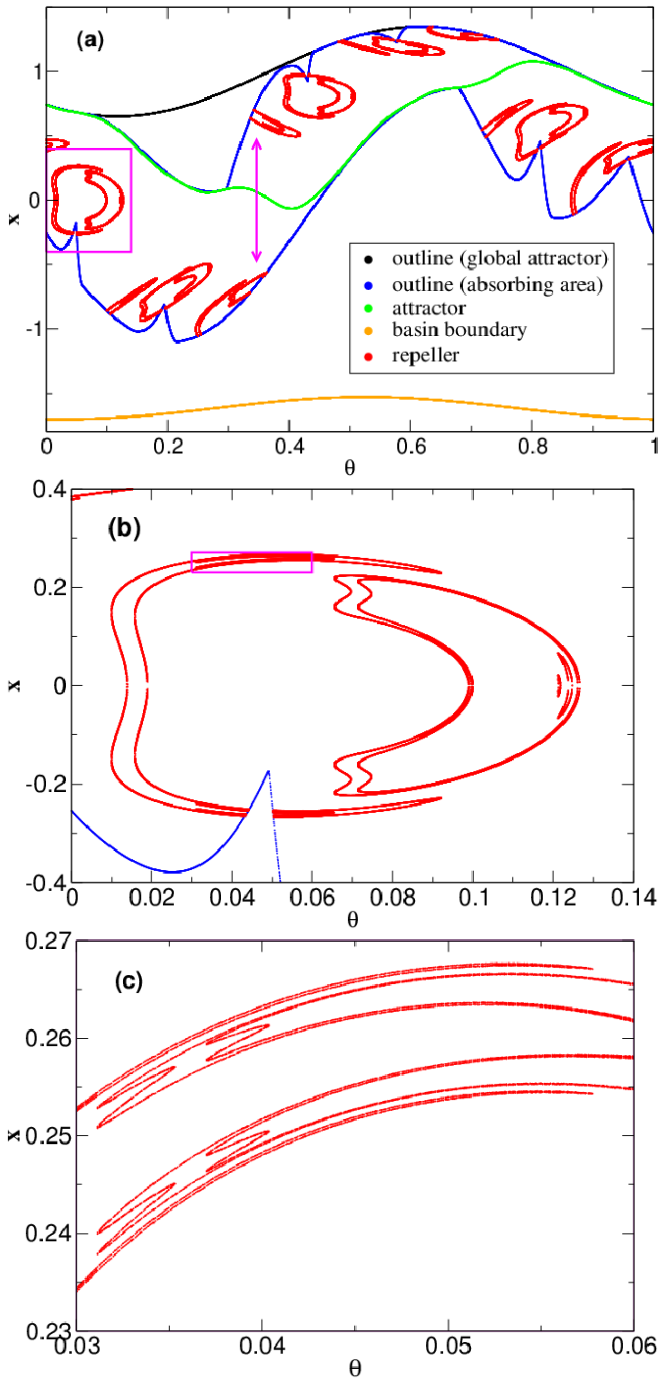


FIG. 2. An example of repeller with non-trivial structure observed at  $(a, \epsilon) = (1.0, 0.35)$ . Thin apertures in the rim of ring like structures are visible in enlarged view in boxes (b) and (c). Data of pull-back attractors and repellers on 10000 target fibers in  $\theta \in [0, 1]$  are used.

#### IV. SUMMARY

We proposed a method to observe a kind of “repeller” in quasi-periodically forced logistic map system and a method to distinguish “smooth” attractors and SNAs,

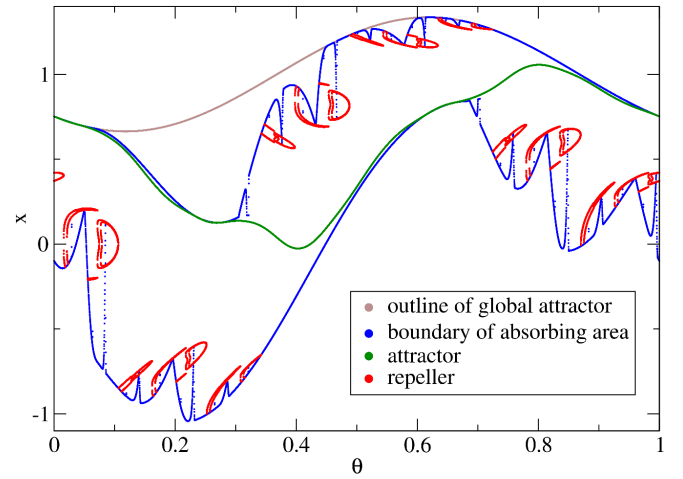


FIG. 3. Repeller and its basin of repulsion, near the emergence of the repeller  $(a, \epsilon) = (1.0, 0.336057731)$ . Data of 10000 target fibers are plotted together.

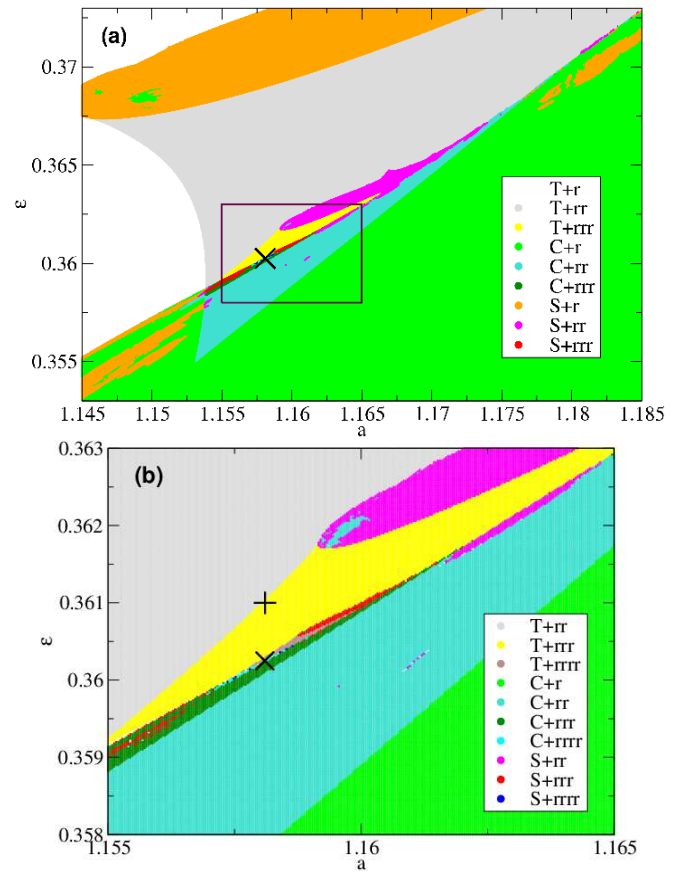


FIG. 4. Phase diagram near TDT critical point  
 Black  $\times$  indicates the TDT critical point  
 $(1.15809685 \dots, 0.36024802 \dots)$  (the value obtained in Kuznetsov et al.<sup>39</sup>). Black  $+$  in box (b) indicates the parameter value used in the next figure. “+rr”, “+rrr” etc. in legends indicate the existence of multiple repellers. These plots are obtained with mesh size  $(\Delta a, \Delta \epsilon) = (0.00004, 0.00002)$ .

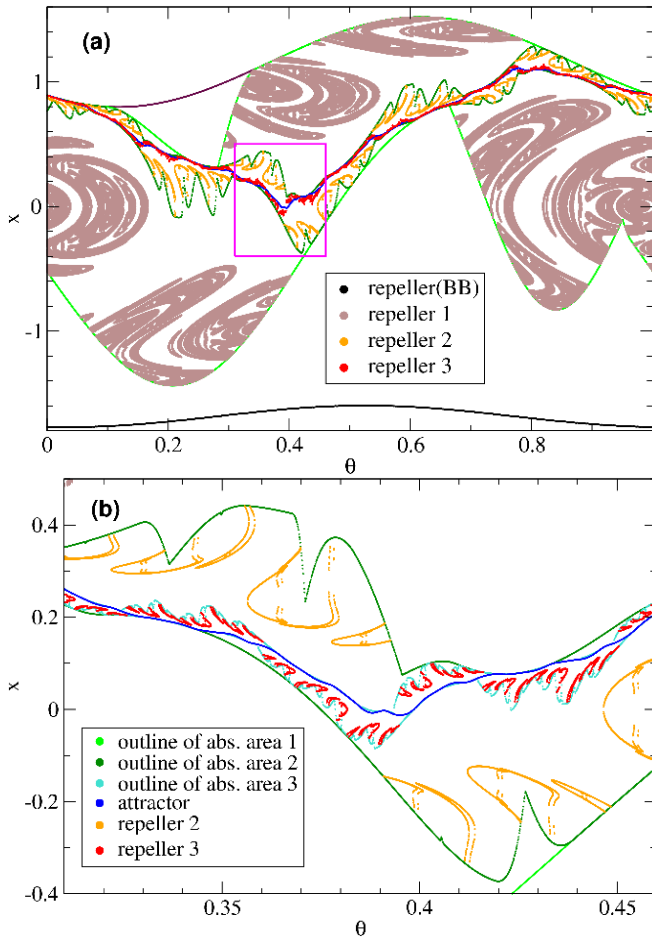


FIG. 5. Nested structure of absorbing areas (basin of repulsion) and corresponding repellers observed at  $(a, \epsilon) = (1.1581, 0.361)$  (indicated by the black + in fig. 4) Plots in box (a), (b) are obtained with 2000, 1500 target fibers of  $\theta$  values within  $[0, 1]$ ,  $[0.31, 0.46]$  respectively.

using auxiliary dynamical system describing evolution of a “line segment” on a fiber. This method enables to obtain images of repellers and bifurcation diagrams efficiently.

Some numerical results obtained with these methods are exhibited, namely,

- phase diagram with some revision in the borderline between smooth torus attractor and SNA,
- detailed images of a repellers with non-trivial ring-like structure,
- absorbing area surrounded by curves with many peaks observed nearly at the emergence of a non-trivial repeller, which exhibits a symptom of non-uniform saddle-node bifurcation in the segment map system,
- nested structure of multiple absorbing areas and associated multiple repellers observed near TDT critical point,

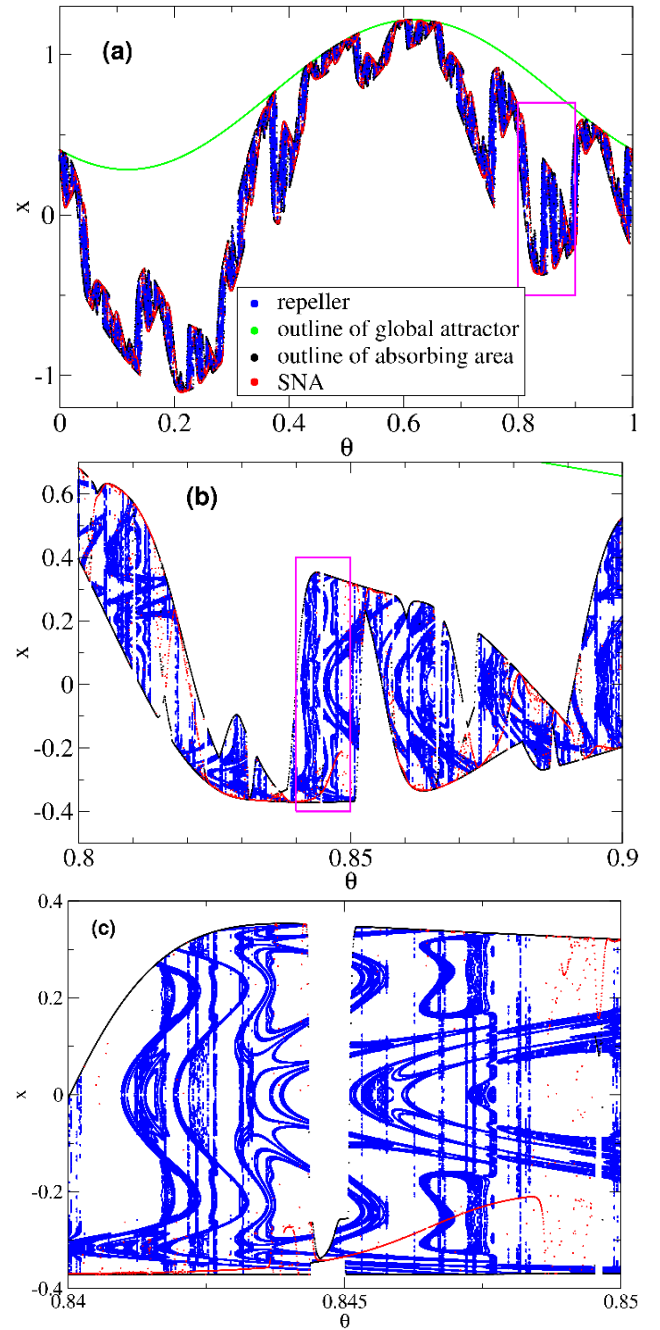


FIG. 6. Repeller and SNA emerged via fractalization route,  $(a, \epsilon) = (0.75, 0.46673)$ . The pull-back attractor (SNA) and the repeller, as well as boundary of absorbing areas, are plotted for 4000 (a), 2000 (b and c) target fibers, with  $\theta$  values in  $[0, 1]$  for (a),  $[0.8, 0.9]$  for (b), and  $[0.84, 0.85]$  for (c) respectively.

- image of repeller with apparently noisy structure which is the counterpart of SNA.

By the use of segment map a similarity between attractors with riddled basin and SNAs become apparent, and the relevance between various phenomena including “fractalization of torus” and “emergence of ring-

like shaped repeller” and (easily observable) bifurcations in the segment map (i.e., bifurcations accompanied with qualitative changes of attractors) are also indicated.

At parameter values where the “fractalization” occur, it seems that the transformation from a smooth torus to SNA and the emergence of a new repeller occur simultaneously. We will report detailed analysis on this phenomenon in the forthcoming paper.

Our method make the most of the fact that the dynamics on the fiber is one dimensional map. Thus it would not be straight forward to apply our method to systems with higher dimensional fiber dynamics. On the other hand, the dynamics of the forcing could be easily generalized, for example, to chaotic ones. As the attraction to SNA in quasi-periodically forced systems could be regarded as a special class of the weak generalized synchronization phenomena<sup>41-43</sup>, application of our method to systems with chaotic driving would help to obtain some new perspective for generalized synchronization phenomena between non-identical chaotic elements.

We appreciate N. Takahashi, T. Mitsui, and Y. Sato for helpful suggestion and discussion. This research is supported by JSPS KAKENHI Grant Number 60115938.

## Appendix A: numerical algorithm

Here we describe some details of the algorithm used in our numerical calculation. Our calculation consists of 3 parts. (1) Search for the invariant sets with nested structure, which gives information of the existence/absence of repellers. (2) Decomposition of the invariant sets into the repeller and the basin of smaller attracting invariant sets, to obtain the approximate images of the repellers. (3) Check for the behavior of perturbed orbits starting from a point on the attractors obtained in (1), in order to distinguish “smooth” attracting torus and SNA. Both (2) and (3) need the result of (1), but (2) and (3) could be carried out mutually independently.

In part (1), we fix a target fiber and will make a list of pull back attractors of  $\tilde{M}$  on the fiber. Here we intend to list up all the attractors that may attract some of the sufficiently short vertical segments. The obtained list would contain those corresponding to the basin of repulsion of repellers as well as those directly corresponding to the attractors of  $M$ . Each of the obtained pull-back attractors is represented by a segment on the fiber (whose length might be zero). In this step, we use evolution towards the target fiber from sufficiently long ago.

In part (2), we choose multiple target fibers that can be reached by forward iteration from the fiber chosen in (1). For each target fiber, we locate the images of the segments obtained in (1) and then try to decompose them to obtain the images of the repellers on the fiber. In the decomposition, we use forward iteration from the target fiber.

In part (3), we choose the zero-length segments obtained in (1) that represent pull-back attractors with neg-

ative lyapunov exponent, and calculate forward trajectory from each of the segments using segment map with small perturbation to  $w$  component. We also calculate the forward iteration starting from segments that correspond to the basin of repellers that possibly has contact with the attractor in question. If these trajectories coincide after sufficiently long transient steps, that indicates the existence of a fiber on which the distance between the attractor and the repeller is smaller than the amplitude of the perturbation, which could be regarded as a signature of the absence of the asymptotic stability of the attractor, implying that the attractor would presumably be an “SNA”.

In the following, we try to illustrate outline of the algorithm in the form of a pseudo program.

```
global variables (for parameters):
  Iinit: a segment on the initial fiber
         chosen so that any invariant set has
         non empty intersection with this segment)
  TList: set of integer
         used to specify theta values of fibers to
         be observed
```

```
global variables (for results):
  InvList: set of segments
           list of pull-back attractor of the
           segment map on the target fiber of Part1
  Unity[J] (J: a member of InvList): boolean
           true if the invariant set represented
           by J do not have proper subset which is
           an attracting invariant set
  RepellerImage[J,t]
           (J: a member of InvList,
            t: a member of TList): set of segments
           image of a section of repeller
           whose basin of repulsion corresponds to J
  SNA[J] (J : a member of InvList): boolean
           true if J is classified as SNA
```

```
working variables:
  I*,J*,K*: segments on a fiber
  I*: on initial fiber
  J*: on target fiber
  K*: on future fiber
```

a. *Part 1: Search for the attracting sets of  $\tilde{M}$*

```
Part1Main
  clear InvList
  call P1CheckImage(Iinit)

Procedure P1CheckImage(I)
  J=IntialTransient(I)
  if (J is not in InvList)
  then
    append J in InvList
    if length(J)>0
```

```

    then
        Unity[J]=P1UnityCheck(I,J)
    else
        Unity[J]=true
if ( (Unity[J] is false)
    and (length(I) > param_cutoff) )
    then
        divide I into (I_1, I_2)
        call P1CheckImage(I_1)
        call P1CheckImage(I_2)
boolean P1UnityCheck(I,J)
"Take an arbitrary point v in segment I"
if ("LyapunovExponent(v)"<0)
    then
        return false
"Take a segment V, as
theta(V)=theta(J),
center(V)=InitialTransient(v),
length(V)=very short"
if (IterateMany(V) and
    IterateMany(J) coincide)
    then
        return true
    else
        return false

```

In this part, we try to obtain a list of pull back attractors of  $\tilde{M}$  on a target fiber. We are interested in such attractors which are also attractors of  $M$  (i.e., stable torus/tori, SNA, chaotic attractor) or which attract orbits with initial conditions that correspond to short segments representing sufficiently small neighborhoods of a point on repellers of  $M$ .

Let the target fiber be specified as  $\{\theta = \theta_0\}$  ( $\theta_0 \in [0, 1)$ ),  $C_-$  be a constant satisfying  $a - C_-^2 + \epsilon < C_-$ , and  $\tau^-$  be a sufficiently large integer parameter that gives the duration of initial transient. Then we take "initial segment" (a point in  $\tilde{\Omega}$ )  $I_{init} = (\theta_-, 0, |C_-|)$  on the initial fiber specified with  $\theta_- = (\theta_0 - \tau^- \omega) \bmod 1$ . With this choice of  $I_{init}$ , every invariant set of  $M$  should have non-empty intersection with  $I_{init}$ .

We calculate the trajectory starting from a segment  $I$  (which is set as  $I_{init}$  for the first trial) on the initial fiber to obtain its image ( $J$ ) on the target fiber, then record  $J$  as a member of the list of pull back attractor on the target fiber ("InvList"). If it has non-zero length and does not correspond to "transitive" chaotic attractor, it is presumed that there exist pull back attractor(s) which corresponds to a proper subset of  $J$ . In such case, we divide the initial segment  $I$  into two, and recursively repeat this calculation with using each fragment of  $I$  as initial segment, until the initial segment becomes sufficiently short.

*b. Part 2: Visualization of repellers*

```

Part2Main
foreach J in InvList
    if (Unity[J] is false)

```

```

    then
        foreach t in TList
            clear tmpRepellerImage
            JT="Iterate_t_times(J)"
            call P2Decomposition(JT)
            RepellerImage[J,t]=tmpRepellerImage

```

```

Procedure P2Decomposition(J)
    K=IterateManytimes(J)
    call P2DecompSub(J,K)

```

```

Procedure P2DecompSub(JX,K)
    L=IterateManytimes(JX)
    if (L matches K)
        then
            if (length(JX)<param_cutoff)
                then
                    "append JX to tmpRepellerImage"
                else
                    "divide JX into (JX1,JX2)"
                    call P2DecompSub(JX1,K)
                    call P2DecompSub(JX2,K)

```

In this part, we choose multiple target fibers, and try to obtain the image of each repeller on each target fiber. The target fibers are chosen to be located on the future of the target fiber of part 1.

We firstly obtain a segments ( $J$ ) on the target fiber that corresponds to the basin of a repeller, and also its image in a sufficient future ( $K$ ). Then divide the segment on the target fiber and check if the image of the fragment in the future is expanded up to coincide with the image of the original segment. If their images in the future matches, it implies that the fragment possibly contains point(s) of the repeller, and in such case we recursively divide the fragments again and check their future image. After a sufficient number of recursive dividing of the segment, we would obtain an approximate image of the repeller on the fiber, i.e., a set of sufficiently short fragments that covers the intersection of the repeller and the target fiber.

*c. Part 3: Sensitivity check for discriminating SNA and torus*

```

Part3Main
foreach J in InvList
    if (length(J) > 0)
        then
            SNA[J]=false
            K[J]=IterateManytimes(J)
foreach J in InvList
    if (length(J) is 0)
        then
            L[J]=PerturbedIterateManytimes(J)
            if (L[J] matches one of K[*])
                then
                    SNA[J]=true
            else

```



SNA[J]=false

In this part, we try to discriminate SNA from smooth torus by checking the sensitivity of final state against a perturbation in a small neighborhood of the attractor.

We calculate a sufficiently long trajectory of perturbed map  $M^+$  starting from a segment (which is the member of InvList in question). If the segment corresponds to an asymptotically stable attractor (i.e., smooth torus/tori attractor), the perturbation would not kick the trajectory out of the basin of the original attractor, but if it corresponds to an SNA, the trajectory would be attracted to another attractor corresponding to the basin of a repeller after a sufficiently long iteration.

Note that the perturbation  $\tilde{W}^+$  affects the map only in a neighborhood of  $\{w = 0\}$  plane, thus attractors detached from  $\{w = 0\}$  are not affected by the perturbation.

- <sup>1</sup>C. Grebogi, E. Ott, S. Pelikan and J. A. Yorke, *Physica D*, 13, 261 (1984)
- <sup>2</sup>K. Kaneko, *Prog. Theor. Phys.*, 71, 282 (1984)
- <sup>3</sup>K. Kaneko, *Prog. Theor. Phys.*, 71, 1112 (1984)
- <sup>4</sup>U. Feudel, S. Kuznetsov and A. Pikovsky, *Strange nonchaotic attractors*, (World Scientific, Singapore, 2006)
- <sup>5</sup>M. Ding, C. Grebogi and E. Ott, *Phys. Rev. A*, 39, 2593 (1989)
- <sup>6</sup>A. Prasad, V. Mehra and R. Ramaswamy, *Phys. Rev. E* 57, 1576 (1998)
- <sup>7</sup>A. Prasad, A. Nandi and R. Ramaswamy, *Int. J. of Bif. and Chaos*, 17 3397 (2007)
- <sup>8</sup>D.V. Senthilkumar, K. Srinivasan, K. Thamilmaran and M. Lakshmanan, *Phys. Rev. E*, 78, 066211 (2008)
- <sup>9</sup>T. Mitsui, S. Uenohara, T. Morie, Y. Horio and K. Aihara, *Phys. Lett. A*, 376, 1907 (2012)
- <sup>10</sup>K. Suresh, A. Prasad and K. Thamilmaran, *Phys. Lett. A*, 377, 612 (2013)
- <sup>11</sup>B.R. Hunt and E. Ott, *Phys. Rev. Lett.*, 87, 254101 (2001)
- <sup>12</sup>J-W. Kim, S-Y. Kim, B. Hunt and E. Ott, *Phys. Rev. E*, 67, 036211 (2003)
- <sup>13</sup>T. Jäger, *Mem. Am. Math. Soc.* 945, 1 (2009)
- <sup>14</sup>G. Keller, *Fundamenta Mathematicae*, 151, 139 (1996)
- <sup>15</sup>T. Yalçınkaya and Y-C. Lai, *Phys. Rev. E*, 56 1623 (1997)
- <sup>16</sup>H.L. Yang, *Phys.Rev. E*, 63, 036208 (2001)
- <sup>17</sup>P. Glendinning, *Discrete and Continuous dynamical systems-series B*, 6, 1 (2002)
- <sup>18</sup>P. Glendinning, *Dynamical systems*, 17, 287 (2002)
- <sup>19</sup>L. Alsedà and M. Misiurewicz, *J. of Difference Equations and Applications*, 14, 1175 (2008)
- <sup>20</sup>K. Bjerklöv, *Nonlinearity* 25, 1537 (2012)
- <sup>21</sup>K. Bjerklöv, *Commun. Math. Phys.* 286, 137 (2009)
- <sup>22</sup>R. Badard, *Chaos*, 18, 023127 (2008)
- <sup>23</sup>P. Glendinning T. Jäger and G. Keller, *Nonlinearity*, 19, 2005 (2006)
- <sup>24</sup>P. Glendinning, T. Jäger and J. Stark, *Nonlinearity*, 22, 835 (2009)
- <sup>25</sup>A. Pikovsky and U. Feudel, *Chaos*, 5, 253 (1995)
- <sup>26</sup>P.R. Chastell, P.A. Glendinning and J. Stark *Phys Lett. A* 200, 17 (1995)
- <sup>27</sup>J. F. Heagy and S. M. Hammel, *Physica D*, 70, 140 (1994)
- <sup>28</sup>T. Nishikawa and K. Kaneko, *Physical Review E*, 54, 6114 (1996)
- <sup>29</sup>A. Witt, U. Feudel and A. Pikovsky, *Physica D*, 109, 180 (1997)
- <sup>30</sup>A. Prasad, V. Mehra and R. Ramaswamy, *Phys. Rev. E*, 79, 4127 (1997)
- <sup>31</sup>U. Feudel, A. Witt, Y-C. Lai and C. Grebogi, *Phys. Rev. E*, 58, 3060 (1998)
- <sup>32</sup>S-Y. Kim, W. Lim and E. Ott, *Physical Review E*, 67, 056203 (2003)
- <sup>33</sup>H. M. Osinga and U. Feudel, *Physica D*, 141, 54 (2000)
- <sup>34</sup>S-Y. Kim and W. Lim, *Phys. Lett. A*, 334, 160 (2005)
- <sup>35</sup>W. Lim and S-Y. Kim, *J. of Korea. Phys. Soc.*, 47, 414 (2005)
- <sup>36</sup>P.E. Kloeden and M. Rasmussen, *Nonautonomous Dynamical Systems, Mathematical Surveys and Monographs*, 176, AMS (2011)
- <sup>37</sup>R. Sturman and J. Stark, *Nonlinearity* 13, 113 (2000)
- <sup>38</sup>J.C. Alexander, J.A. Yorke, Z. You and I. Kan *Int. J. Bifurcation Chaos* 2, 795 (1992)
- <sup>39</sup>S. Kuznetsov, A. Pikovsky and U. Feudel, *Phys. Rev. E*, 51, R1629 (1998)
- <sup>40</sup>S. Kuznetsov, *Phys. Rev. E*, 72, 026205 (2005)
- <sup>41</sup>T.U. Singh, A. Nandi and R. Ramaswamy, *Phys. Rev.*, E 78, 025205 (2008)
- <sup>42</sup>G. Keller and A. Otani, *Dynamical Systems*, 28, 2 (2013)
- <sup>43</sup>G. Keller, H.H. Jafri and R. Ramaswamy, *Phys. Rev. E*, 87, 042913 (2013)
- <sup>44</sup>J. Chubb, E. Barreto, P. So and B.J. Gluckman, *Int. J. of Bifurcation and Chaos*, 11, 2705 (2001)